Arab Gulf Journal of Scientific Research, 24 (2), pp 83-93 (2006)

Original Paper Ref. No . 2331

Geophysical Investigation of Groundwater in Wadi Lusab, Haddat Ash Sham Area, Makkah Al-Mukarramah

دراسات جيوفيزيائية للمياة الجوفية في وادي اللصب، منطقة هدا الشام، مكة المكرمة

منصور القرني، حمدي حسنين و محمد غباشي

[1] ***M. Al-Garni, H. Hassanein and M. Gobashy***

Department of Geophysics, Faculty of Earth Sciences, King Abdul Aziz University
P.O. Box 80206, Jeddah, 21589, Kingdom of Saudi Arabia.
[1] To whom correspondence should be addressed: E-mail: maalgarni@kau.edu.sa

Abstract: Schlumberger sounding and ground magnetic surveys were conducted in Wadi Lusab, Hadat El-Sham area, to examine the possible existence of groundwater and structures that may control water flow. Schlumberger soundings were made along and across the Wadi Lusab. The Schlumberger sounding curves were generally of good quality; however, a few sounding curves were affected by lateral geologic inhomogeneities and man-made objects which may have distorted others. The interpreted resistivity sounding curves, cross-sections show a clear picture of the probable location of the water table, the water quality, and possible structure of the studied area. Materials with resistivities (150 to > 300 ohm-m) may represent dry alluvial deposits of sand and gravel and pebbles. Materials with resistivities (70 to 150 ohm-m) may represent sedimentary deposits of coarse sand and gravel saturated with good quality water. Materials with resistivities (30 to 70 ohm-m) may represent deposits composed of sand and gravel mixed with clay and probably saturated with good quality water. Materials with resistivities (10 to 30 ohm-m) may represent sedimentary deposits with a medium percentage of clay mixed with sand and gravel saturated with good quality water. Three interpreted resistivity cross sections illustrate the above findings. The ground magnetic survey, on the other hand was conducted along Wadi Lusab. It delineates the major faults and estimates the thickness of sedimentary cover. Possible existence of faults across the Wadi was confirmed by magnetic sources obtained from the application of Euler homogenity equation to the observed profile. The magnetic interpretation shows that the thickness of the sedimentary cover in the western part of the studied area is greater than the eastern part. The western part of Wadi lusab shows a system of potential faults that may affect the water flow. A profile of interpreted magnetic data illustrates the above findings.

Keywords: Ground water, geophysical, Schlumberger sounding, ground magnetic, surveys, Makkah, Saudi Arabia.

المستخلص: في هذا البحث تم عمل مسح كهربي باستخدام طريقة شلمبرجير ومسح مغناطيسي ارضي في وادي اللصب بمنطقة هدى الشام بمنطقة مكة المكرمة وذلك لاستكشاف إمكانية وجود خزان مياه جوفي والتركيبات البنائية التحت سطحية التي ربما تتحكم في سريان المياه بالمنطقة . تم تنفيذ المسح الكهربي بواسطة طريقة شلمبرجير على طوال وبعرض الوادي وكانت نتائج غالبية المنحنيات الكهربية الناتجة ذات مدلولات جيدة أما البعض الآخر فلقد تأثر إما بالتركيبات الجيولوجية المعقدة بالمنطقة أو المنشات الصناعية مما أدى إلى التقليل من جودة نتائج المنحنيات . وبصفة عامة أعطت نتائج الطرق الكهربية بعد تفسيرها صورة واضحة لاماكن ومستوى الخزان الجوفي بالوادي بالإضافة إلى تحديد جودة المياه لهذا الخزان والأشكال البنائية المعترضة له والتي ربما تؤثر عليه . وأوضحت أن المواد ذات المقاومية الكهربية ما بين 150 إلى > 300 اوم -م تمثل غالبا ترسبات وادي جافة تتكون من الرمال والحصى إما المواد ذات المقاومية الكهربية من 70 إلى 150 اوم - م فهي تمثل غالبا رسوبيات من حصى ورمال اكبر نسبيا في الحجم مشبعة بالمياه وهذه المياه عالية الجودة . إما المواد ذات المقاومية من 30الى 70 اوم - م فتمثل رسوبيات مكونة من الرمال والحصى مخلوطة ببعض الطفله وغالبا ما تكون مشبعة بالمياه ذات الجودة العالية . وفي النهاية المواد ذات المقاومية الكهربية من 10 إلى 30 اوم - م تمثل ترسبات ذات نسبة متوسطة من الطفلة مختلطة برمال وحصى مشبع بمياه ذات جودة جيدة . وقد أوضحت ذلك المقاطع الكهربية المفسرة . أما بالنسبة للمسح المغناطيسي الأرضي فلقد تم تنفيذه على طوال الوادي وأكد وجود فوالق وصدوع وحدد تقريبا سمك الغطاء الرسوبي بالوادي وأمكن الحصول على مصادر الشاذات المغناطيسية بالمنطقة بتطبيق معادلة اويلر المتجانسة على البيانات المأخوذة حقليا . وأوضح تفسير النتائج إن سمك الغلاف الرسوبي في المنطقة الغربية اكبر منه عن المنطقة الشرقية وان الجزء الغربي من الوادي واقع تحت تأثير مجموعة من الصدوع التي ربما تؤثر على سريان الماء الجوفي بالوادي ..وتم عرض تفسير كمي للبيانات المغناطيسية على طوال الوادي.

كلمات مدخلية: مسح كهربي ، طريقة شلمبرجير، مسح مغناطيسي، المياه الجوفيه، مكة المكرمة، المملكة العربية السعودية.

Introduction

The Haddat Ash Sham area lies at the intersection of 21° 49.1' N latitude and 39°43.6 E longitude. It has an average altitude of 330 m is approximately 100 km to the east-northeast of Jeddah and is considered as a part of the Usfan catchment (Fig. l). It is one of the most important vegetation areas in Makkah Al-Mukarramah region.

With the increase of groundwater for public supply, and irrigation use, research and exploration were needed to find new resources of good quality water in Wadi Lusab for the Makkah Al-Mukarramah region. Wadi Lusub is the main stream in Haddat Ash-Sham area. It drains both the Wadi Madrakah and the Wadi Zabyah, that initiates from the plateau of Harrat Rahat and runs southwesterly entering the Usfan plain 5 km down stream of the Hadat Ash Sham village. The area lies within a typical arid region.

Bahafzalla *et al.* (1983) showed that the sedimentary sequence exposed in the study and surroundings areas consists of Cretaceous-Tertiary sedimentary succession, Tertiary-Quaternary, Basaltic lava flows, and Quaternary-Recent alluvial deposits (Table 1). Al Shanti *et al.* (1966) and Moore and Al Reheili (1989) delineated that the basement complex rock units of this area consist of Late-Proterozoic basaltic to rhyolitic volcanic, volcanoclasitc, and epicalstics of primitive island-arc type. These basement complex unites have been multiply deformed, metamorphosed, and injected by intrusive bodies of different ages and compositions (Fig. 2).

The Cretaceous-Tertiary sedimentary rock units include the Haddat Ash Sham, Usfan, and Shumaysi formations as shown in Table 1. Moore and Al-Rehaili (1989) grouped these sedimentary rock units in three NNW trending asymmetric depositional troughs. Bahafzalla *et at.* (1983) showed that the Haddat El-Sham Formation of Cretaceous age has a thickness of approximately 250 m. Zeidan and Banat (1990 A) showed that its beds are dipping to the Northeast at an angle of 10°-18°.

Smith (1981, 1982) mapped the Cenozoic basaltic rocks of Harrat Rahat, which extends to the North of the study site area, from Al-Madinah Al-Munawarah southward for about 310 km. Quaternary deposits occur in the drainage basin of Haddat Ash Sham and neighboring basins. The principal units of Quaternary rocks are the terrace gravel, alluvial fan deposits, talus deposits, alluvial sands, gravels of Wadi beds, and some Aeolian edifices with the thickness varying from one place to another.

Wadi Lusab is the main source of water supply for the important vegetation area in the Makkah Al-Mukarramah region. Therefore, the present study aims to delineate the subsurface structures that control the water flow along Wadi Lusab using DC resistivity and ground magnetic methods.

Faults and joints are the prominent structural feature in Wadi Lusab area. The sedimentary layers are mostly dragged or flextured around the fault plane. Generally, these faults show limited extension ranging from 1 km up to 10 km. Most of the faults are highly angle normal faults with small throw. The NE-SW Faults form elongated grabens in southwestern and northeastern parts of the investigated area. Most of the scarps and valleys dissecting the Haddat Ash Sham area are fault controlled (Bahafzalla, *et al.* 1983).

The Precambrian rocks for the area northeast of Jeddah have been affected by polyphase formation events including folding, shearing, and faulting (Moore and Al-Reheili 1989). The Red Sea rift system has affected most of the rock units from the Precambrian to Quaternary and forms three main sets of structural features (NW, NE and N).

El-Dobakhy (1999) studied the ground water level in a number of wells in the study area and concluded it as shown in Table 2. He also described the subsurface geological structure of Hadat Ash-Sham area as a sedimentary layer extending to the surface of the fractured rocks at depth ranges from 26 to 30 m. Other massive basement rocks at depth ranges follow the fractured rocks from 45 to 70 m from the ground surface. They concluded that the depth of ground water surface ranges from 8 to 10 m beneath the ground surface.

Gophysical Survey and Interpretation Techniques

Ground Magnetic Survey

The recent intensified interest in the geology of Makkah Al-Mukarramah region is particularly related to the potential of underground water. The scarcity of information for the area lends to a considerable importance of geophysics and specially the present ground magnetic profile that extends across the major tectonic elements of the Haddat Ash-Sham area. The data was recorded along a profile extending approximately seven kilometers from the upstream to the downstream of Wadi Lusab (Fig. 3). The analysis of the magnetic anomalies approximates the thicknesses of sedimentary overburden within the limitations that inherent from using a single profile.

The proton precession type magnetometer (ENVI-Mag, SCENTRIX) is used to measure the

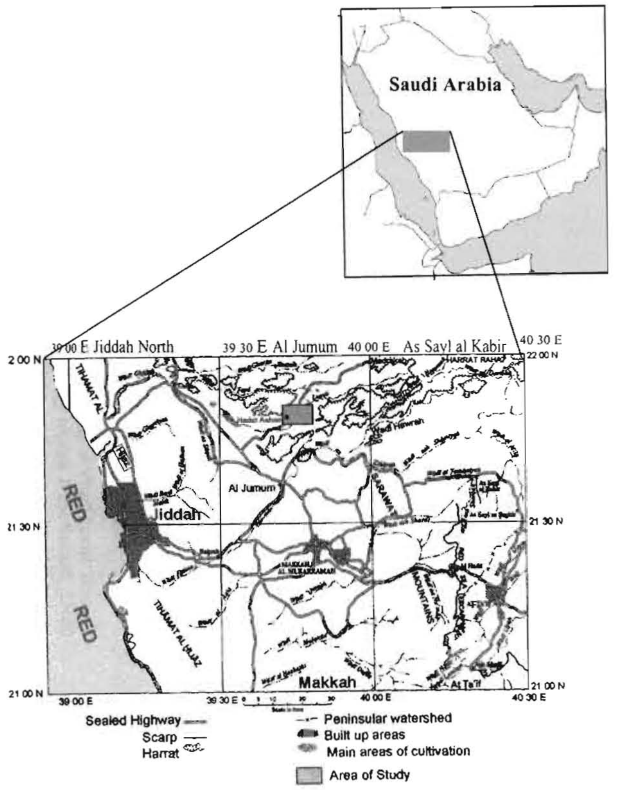

Fig. 1. Location map of the studied area

total magnetic intensity component. A total of 138 readings were recorded and the routine correction of the data was carried out. The total intensity magnetic profile has an arbitrary magnetic datum (Fig. 4a). Smoothing has been applied which eliminates small, short period irregularities of 5 gammas or less that may be considered as combination of equipment noise, slight irregularities introduced in the compilation process, and very minor geologic effects. The profile is quite gentle and has maximum amplitude of 40710 gammas at about 5070 m from the starting point at the upstream side (East). An observable gradient downward to the west of slightly more than 20 gammas/kilometer is observed (Fig. 4b). This gradient is the combined effect of instrumental drift, the diurnal variation, and the component of the earth's main magnetic field along the survey line. The instrumental drift was considered minimum according to the short surveying time of 3.5 hours.

Magnetic Data Processing

The profile can be divided into two major segments, which are labeled on the profile as A and B. The A segment is characterized by minor irregularities of 10 to 15 gammas while on the contrary the B segment is characterized by a major well defined magnetic anomaly of relief of approximately 130 gammas. These variations depend on the subsurface structural variations of the basement surface, which are mainly related to the variation of composition and depth of basement rocks. The main features of high frequency anomalies can be explained by the existence of broad zones of high magnetization in the crystalline rocks beneath the sediments.

In order to quantitatively determine the depth to the causative source of the magnetic anomalies along the profile, a semi automatic Euler deconvolution procedure is applied to the profile. It is appropriate to mention here the Euler's homogeneity equation in 3-Dimension is described as (Reid, *et al.* 1990):

$$(x-x_0)\frac{\partial T}{\partial x}+(y-y_0)\frac{\partial T}{\partial y}+(z-z_0)\frac{\partial T}{\partial z}=N(B-T)$$

Where T (x, y, z) is the total field magnetic in Cartesian co-ordinates, (x_0, y_0, z_0) the co-ordinates of the source, N the Structural Index, and B the regional field.

In the two-dimensional (2-D) case, only terms with x and z are kept while those with y are canceled. The three unknowns in equation (1) in 2-D (B, x_0, z_0) are solved by matrix inversion from an array of nodes along the profile with a predetermined window. Fig. 5a,b,c, shows the original and reduced pole data, the gradients (vertical in red and horizontal in black), and results of all possible solutions, respectively. The crosses in Fig. 5c, represent sources (x_0, z_0) with varying depths. The index parameter is chosen such that N=1, which represents a magnetic contact that is expected in the study area. It is necessary to mention that the results of Euler deconvolution method are generally mapping structural boundaries (e.g. faults and contacts) better than determining depth to basement, which is the main interest of this analysis. Therefore, Fig. 5d shows a possible earth model that has been found from a Euler deconvolution.

Interpretation of Total Intensity of Ground Magnetic Data

The total magnetic intensity curve along the Wadi Lusab showed that recognizable faults or discontinuities dividing and crossing the Wadi area into two parts, the western part is characterized by high frequency magnetic anomalies and the eastern part is characterized by low magnetic relief anomalies with relatively low amplitude and frequency (Fig. 5). These magnetic features indicate that the surface of basement or the depth to

Table 1. Stratigraphic units in Wadi Lusab area

Age	Formation	Lithology	Thickness (m)
Quarternary.	Surficial deposits including alluvial deposits of the Wadi System.	Heterogeneous assemblage of Gravels sands, silt, and clay.	<30
Tertiary Quarternary.	Basalt flows.	Basalt and andesite.	<60
Eocene – Oligocene.	Shuymaysi Formation.	Sandstone, siltstone with oolitic ironstone bands.	20-200
Maestrichtian.	Usfan Formation.	Sandstone , shale, marls, and carbonate ledge.	
Cretaceous.	Haddat Ash-Sham Formation.	Conglomerate, sandstone, Breccia with claystone and siltstone.	250
Cambrian Precambrian.	Basement Complex.	Igneous and metamorphic Complexes.	

magnetic source rocks has an average of about 130 m between 3800 and 5500 m along the profile. The steep gradient which is shown at the distance between 5500 and 6000 m indicates a possible fault occurrence in this zone and no Euler solutions can be detected at the distance greater than 6000m. Also, at the Eastern side (between 0 and 1800 m), the magnetic relief is very low and the Euler solutions are not quite confident, which may reflect either very deep sources or very shallow non-magnetic sources. The central part between 1800 and 3800 m displays sources that are very shallow (approximating 20-30 m) compared to the eastern part. Therefore, the thickness of sedimentary cover in the western part is relatively more than the eastern part and the maximum thickness of the sedimentary cover is probably between 3800 and 5800 m.

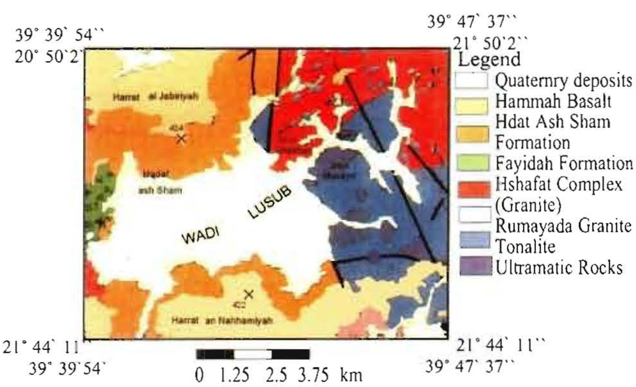

Fig. 2. Geological Map of Wadi Lusub Area. (Modified after Moore and El-Rohaili 1989).

Accordingly, the western part of Wadi Lusab is characterized by a system of faults or boundaries, which affects the water flow from the side of Wadi, which is considered as the upstream side. This part of Wadi is more complex from the point of view of geology and magnetic measurements. As a result of previous discussion, the thickness of sedimentary deposits is enough for underground water storage.

Vertical Electrical Sounding Survey

A total of nine Schlumberger soundings were made at the studied sites (Fig. 3). The maximum expansion of the current electrode spacing (AB/2) reached up to 150 m for some soundings in order to obtain reasonable data continuity and considerable depth penetration. The instrument that was used in conducting the survey is ELREC-T model, IRES made.

The quality of most collected sounding curves are excellent; however, we recognize some of the sounding curves are affected by inhomogenties at short-distance potential electrodes such as sounding 1003 (Fig. 6) and by man-made objects such as sounding curve 1008 (Fig. 7). Two examples are provided in this paper to show how the inhomogentiy and man-made objects affect the resistivity curves and may lead to misinterpreting DC resistivity curves if someone does not recognize them. The first example (Fig. 6) was corrected by changing the affected apparent resistivity reading into a reasonable value, which was assumed from

Table 2. Depths of Ground water level in the study area after Dobakh y (1999).

Ser. No.	Well code no.	Well location.		Depth of water level	Thinness of Saturated layer
		Long.	Lat.		
1	A	39° 43′ 26″	21° 47′ 34″	27	Not defined
2	C	39° 43′ 33″	21° 47′ 35″	26.3	Not defined
3	D	39° 43′ 53″	21° 47′ 44″	15.3	Not defined
4	E	39° 44′ 2″	21° 47′ 54″	16.5	Not defined
5	1	39° 43′ 42″	21° 47′ 9″	12	30
6	2	39° 43′ 33″	21° .47′ 59″	47	35
7	3	39° 43′ 30″	21° 47′ 50″	12	35
8	4	39° 43′ 38″	21° 47′ 43″	15	4
9	5	39° 43′ 49″	21° 47′ 51″	7	18
10	6	39° 43′ 34″	21° 47′ 40″	6	35
11	7	39° 43′ 20″	21° 48′ 2″	6	35
12	8	39° 43′ 49″	21° 47′ 58″	6	35
13	19	39° 43′ 41″	21° 47′ 45″	6	48

the behavior of nearby resistivity values on the same sounding curve or the corresponding AB/2 of the resistivity value of a nearby location in the same area. This correction is made in order to avoid unreasonable interpretations. The second example (Fig. 7) was corrected by truncating the last three readings which may have been affected by a metal fence located at a distance of about 100 m from the center of the array in order to avoid the effect of the artificial objects (Al-Garni, 1996).

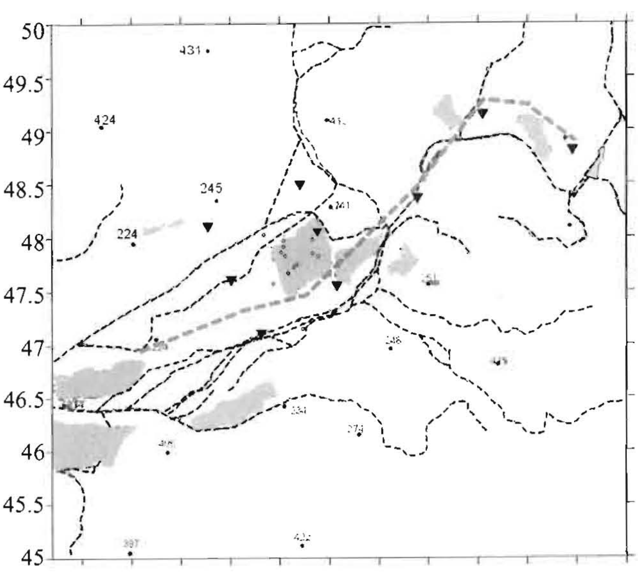

Fig. 3. Location of Electric survey (▼). Ground Magnetic profile ▬ and well sites ○

Vertical Electrical Sounding Processing

The automatic analysis of the vertical electrical sounding curves (VES) is implemented using two methods:

1. The first method used an automatic interpretation computer program (Zohdy and Bisdorf, 1989) where the layering models are shown as step function curves which represent the variation of resistivity with depth (Fig. 8a). This variation is conventionally considered to be beneath the center of the electrode array.

Shifting the various segments on the field curve (which obtained a fixed potential electrode spacing (MN/2)) upward or downward was done in order to construct a continuous smoothed curve. Usually last segment is fixed and all other segments are moved up and down relatively to it. The reason for keeping the last segment fixed is that the measurements at large potential electrode spacing are not affected by small, near surface, laterals inhomogeneity such as boulders (Al-Garni, 1996). Sampling the smoothed curve at the rate of 7 logarithmically equally spaced point per logarithmic cycle was done in order to obtain the digitized curve. This sampling was done from right to left. The reason is that if the length of the shifted sounding curve is not devisable by 7 then the curve will be dropped. The shifted field curve was sampled at the rate of 6 logarithmically equally spaced points per decades in order to speed up the calculation of various theoretical sounding curves during the iterative fitting process (Zohdy, 1974).

Table 3. Results of forwarded modeling along of vertical electrical soundings along profile (Ta).

VES 1007 north				VES 1008				VES 1010 south			
L. no	**Res.**	**Th.**	**Dep.**	**L. no**	**Res.**	**Th.**	**Dep.**	**L. no**	**Res.**	**Th.**	**Dep.**
1	62.3	5.5	5.5	1	129.9	2.0	2	1	1625	1.3	1.3
2	5.7	6.0	11.5	2	72.4	5.3	7.3	2	273.2	3.6	4.9
3	12.1	8.8	20.2	3	18.6	16.1	23.4	3	92.5	7.7	12.6
4	19.2	8.8	29.0	4	15.7	***		4	15.1	11.4	24.1
5	4.6	68.7	97.7					5	14.2	***	
6	43.4	****									

Every point on the theoretical sounding curve is calculated by convolving a set of points on the kernel function curve (Ghosh, 1971; Zohdy, 1975) with a set of filter coefficients. Zohdy and Bisdorf (1989) used the O'Neill filter coefficients (O'Neill, 1975), which are used to calculate the sounding curve at the rate of 7 points per decade.

2. The second method is based on the solution suggested by Davis (1979) using the original concept of Ghosh (1971). This method requires an initial input-layering model. This initial model is modified in resistivities and thicknesses through a number of iterations until the best fit between the calculated resisyivity of the model and the sounding curve is obtained (Fig. 8b). The final layering model of the sounding curves along profiles is shown in Tables 3,4, and 5.

Interpretation of Vertical Electrical Sounding Data

Generally, Groundwater exploration depends on the variation of the resistivity of saturated and unsaturated layers, which maybe also depends on many additional, parameters such as lithology, grain size, clay content, salinity and depth.

Accordingly, three resistivity cross sections were constructed (Figs. 9,10,11). One of these cross sections is oriented E-W direction along Wadi Lusab, and the others are oriented to S-W direction across the Wadi. The interpreted resistivity contours that are shown on the cross sections are derived from the step function layering. Such interpretation provides better distinguished subsurface features of different formations and the possibility of the groundwater occurrences.

Material with very low resistivities (3-10 ohm-m) generally represent sedimentary deposits with a

Table 4. Results of forwarded modeling of vertical electrical soundings along profile (Tb).

1006 north				VES 1009				VES 1005 south			
L. no	**Res.**	**Th.**	**Dep.**	**L. no**	**Res.**	**Th.**	**Dep.**	**L. no**	**Res.**	**Th.**	**Dep.**
1	38.2	1	1	1	164.3	1.2	1.2	1	445.9	1.6	1.6
2	102.6	1.1	2.1	2	458.9	0.6	1.8	2	103.4	2.2	3.8
3	158	2.1	4.3	3	37.8	4.1	5.9	3	50.5	7.5	11.4
4	36.62	9.6	14.2	4	70.3	6.1	12.0	4	23.6	***	
5	10	***		5	43.2	22.1	34.1				
				6	6.9	**					

Table 5. The results of forwarded modeling of vertical electrical soundings along profile (AW).

VES 1001 east				VES 1002				VES 1003 south				VES 1009				VES 1008 south			
L. no	**Res.**	**Th.**	**Dep.**	**L. no**	**Res.**	**Th.**	**Dep.**	**L. no**	**Res.**	**Th.**	**Dep.**	**L. no**	**Res.**	**Th.**	**Dep.**	**L. no**	**Res.**	**Th.**	**Dep.**
1	85.2	1.4	1.4	1	968.0	1.7	1.7	1	113.2	1.7	1.7	1	164.3	1.2	1.2	1	445.9	1.6	1.6
2	42.1	2.2	3.5	2	378.6	4.4	6.1	2	107.9	1.6	3.2	2	458.9	0.6	1.8	2	103.4	2.2	3.8
3	128.1	6.0	9.6	3	212.9	4.2	10.3	3	83.8	6.4	9.7	3	37.8	4.1	5.9	3	50.5	7.5	11.4
4	19.6	12.3	21.9	4	19.7	15.2	25.5	4	22.1	27.3	36.9	4	70.3	6.1	12.0	4	23.6	***	
5	177.9	**		5	230.7	***		5	139.3	***		5	43.2	22.1	34.1				
												6	6.9	**					

high percentage of clay content and may unlikely contain good quality water or represent sand and gravel deposits saturated with brackish to saline water (TDS of 1000 to 10,000 mg/l).

Material with medium low resistivities of (10-30 ohm-m) generally represent sedimentary deposits with a lower percentage of clay mixed with sand and gravel and may be saturated with good quality water.

Material with medium resistivities (30-70 ohm-m) may represent sedimentary deposits of fine sand and gravel mixed with low percentage of clay and saturated with good quality water (less than 1000 mg/l of TDS).

Material with medium high resistivities (70-150 ohm-m) may represent alluvial deposits with coarse sand and gravel saturated with good quality water (probably less than 500mg/l of TDS).

Material with high resistivities (150 to larger than 300 ohm-m) may represent unsaturated near surface sand, gravel, and cobbles that are usually found in the top of the parts of the alluvial fans.

The interpretation of vertical subsurface resistivity contour section (Figs. 9,10,11) was constructed after a careful examination of the resistivity contour behavior. The contour gradient was used to locate the boundary between two geoelectric layers, while the closed contour was used to describe the thickness of any interpreted layer. Using these criteria, it was possible to obtain an equivalent subsurface geoelectric configuration, which can be expressed by the lithological model superimposed on the contour sections.

The geoelectric section (A), along Wadi, indicates the variation in depth level and the occurring of the two layers, arising from the fault affecting area at the west of VES No.1003 (Fig. 9). The geoelectric sections (Ta and Tb) across the Wadi indicate that there is a Variation in distribution of ground water from S to N and according the resisitivity values also are varied (Figs. 10, 11).

Tables 3,4, and 5 show the results of forward modeling along of vertical electrical soundings along profile A, Ta, and Tb, respectively. Along profile Ta, the thickness of low resistivity layer increases reaching 92.2 m beneath VES 1007. The observed resistivity delineates that the depth of the water table beneath the location of VES 1008 and VES 1010 are 23.4 and 24.1, respectively.

The depth of the lower boundary of the water bearing formation is not defined. Along profile Tb, the thickness of low resistivity layer beneath VES 1005 and 1006 are 9.6 m and 7.5 m, respectively at depths 11.4 and 14.2 m from the ground surface. The observed depth beneath the lower resistivity

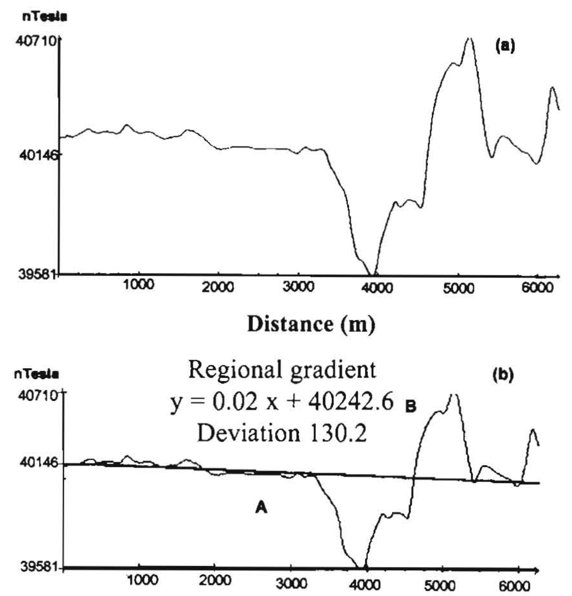

Fig. 4. a) Total intensity magnetic curve along Wadi Lusab, Hadat Ash Sham, Makkah Almokaramah region, Saudi Arabia. b) The regional magnetic trend as subtracted from the main field.

layer may correspond to the surface of the ground water which is of about 5.9 m. The resistivity below this depth ranges between 6.9 m to 70m and may return to the variation of saturation and lithological properties of bearing water formations.

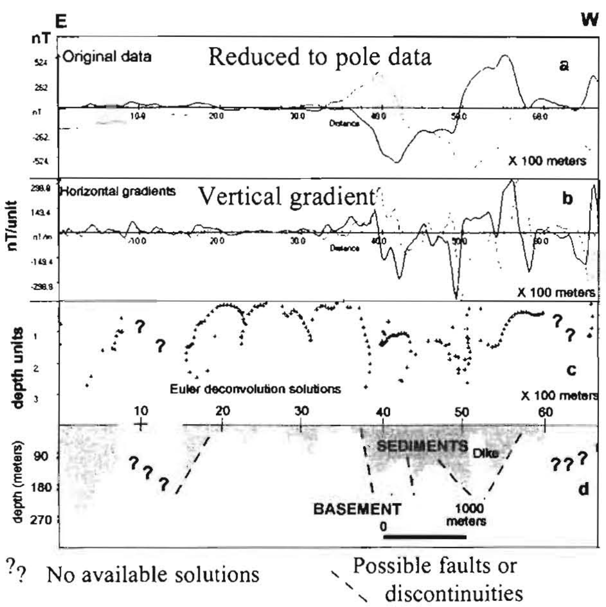

Fig. 5. Euler deconvolution solution depths for Land magnetic profile, Hada Asham Area, Mekkah, SA
a) both observed and reduced to pole (RTP) fields,
b) The horizontal and vertical gradient fields,
c) The Euler deconvolution solution depths, and
d) a possible earth model as composed from Euler depths and geologic information available.

Conclusions

The interpretation of resistivity cross section TA showed that the middle and the northern part of the studied profile most probably contains substantial sand and gravel saturated with good quality water. The southern part of the studied profile, cross section TA, most probably contains fine sand and clay deposits saturated with good quality water also. The interpretation of resistivity cross section TB showed that the middle and likely the southern part of the studied profile most probably contain sand and gravel saturated with good quality water. The northern part of the studied profile, cross section TB, most probably contains fine sand and clay deposits saturated with good quality water. The interpretation of resistivity cross section A, which was taken along the Wadi, showed that the eastern part of the profile most probably contains substantial sand and gravel saturated with good quality water and gradually to the west most probably contains sand and less gravel saturated with good quality water.

Ground magnetic analysis showed that the basement has an average depth of about 130 m between 3800 and 5500 m, a possible fault between 5500 and 6000m, and a shallow basement depth of about 20-30 m in the central part of the profile. Therefore, the sedimentary deposits in the eastern part are relatively less than the western part and the thicker sediments maybe located between 3800 and 5800 m.

The integration between the DC resistivity method and the magnetic method reveal a better understanding for the possible groundwater configuration, depth to basement lateral variations within the varying subsurface layers, and the local subsurface structures.

References

Al-Garni, M.A. (1996) Direct current resistivity investigation of groundwater in the Lower Misilla Valey, New Mexico and Texas, M.Sc. thesis, Colorado School of Mines.

Al Shanti, (1966) Oolitic iron ore deposits in Wadi Fatima between Jeddah and Makkah, Saudi Arabia: Saudi Arabia Directorate general of mineral resources, Bull. 2, pp 686-696.

Bahafzalla, A, Basahal, A.N., Mansour, H.H., and Omara, S. (1983) Geologic Mapping and stratigraphy of the swdimentary sequence in Haddat Ash Sham area, northern of Jeddah. Vol.1, No. 2, pp 423-442.

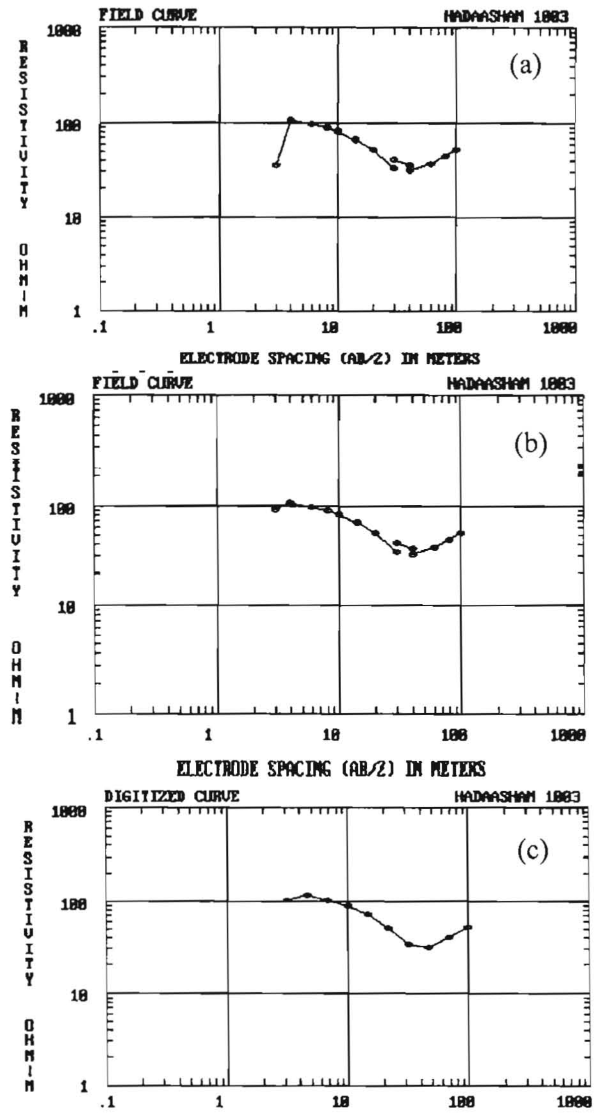

Electrode spacing (AB/2) m

Fig. 6. The original VES curve (a), The modified VES Curve (b) and the final digitized curve (c) of the VES 1003.

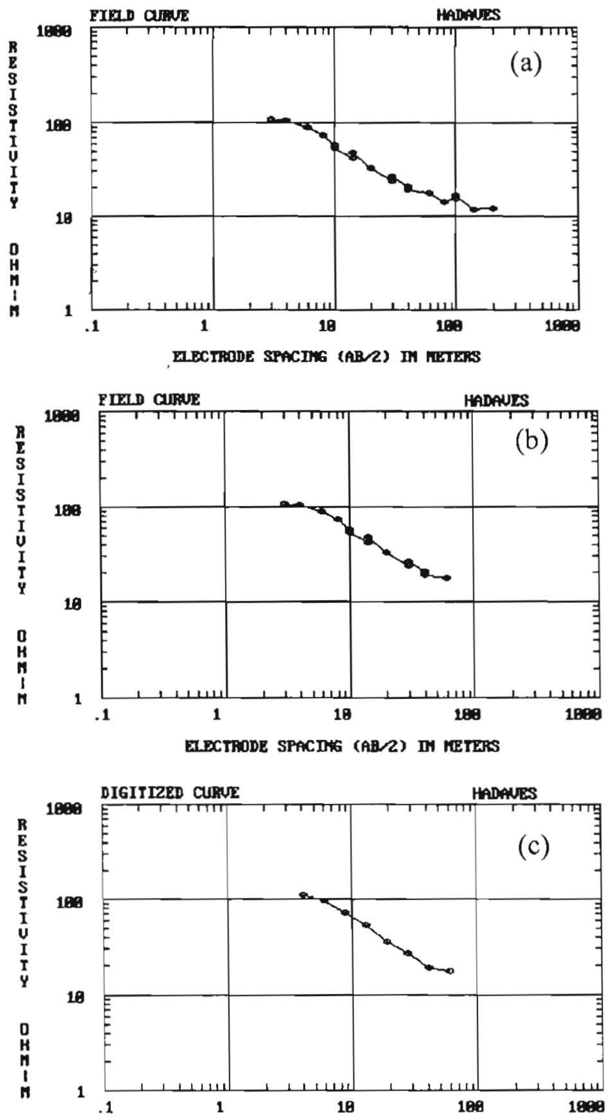

Electrode spacing (AB/2) m

Fig. 7. The original VES curve (a), The modified VES Curve (b) and the final digitized curve (c) of the VES 1008.

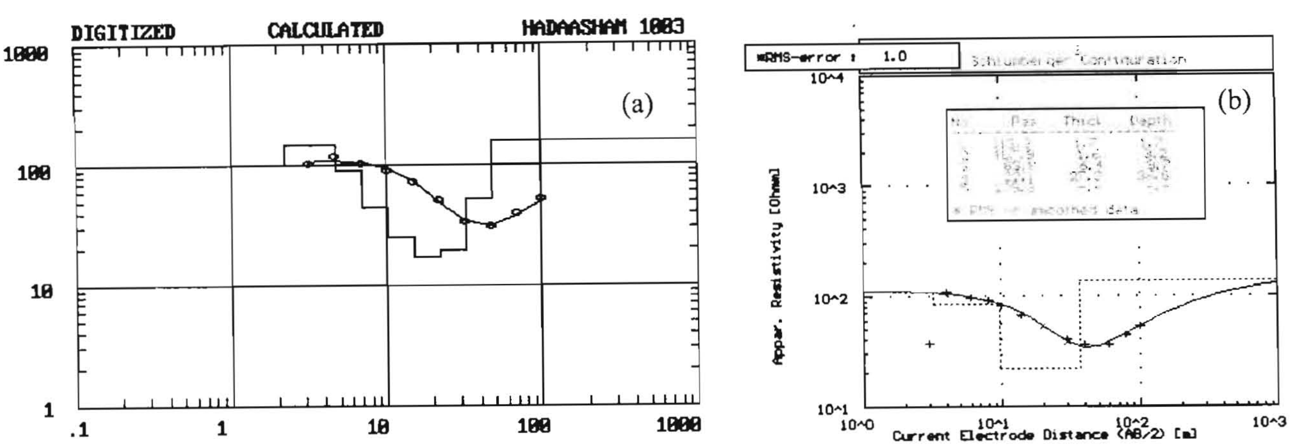

Electrode spacing (AB/2) or depth (m) **Current Electrode Distance (AB/2) (m)**

Fig. 8. Example on the sounding analysis of VES-1003 using (a) Zohdy Method (1975 and 1989) (b) Merrick (1977).

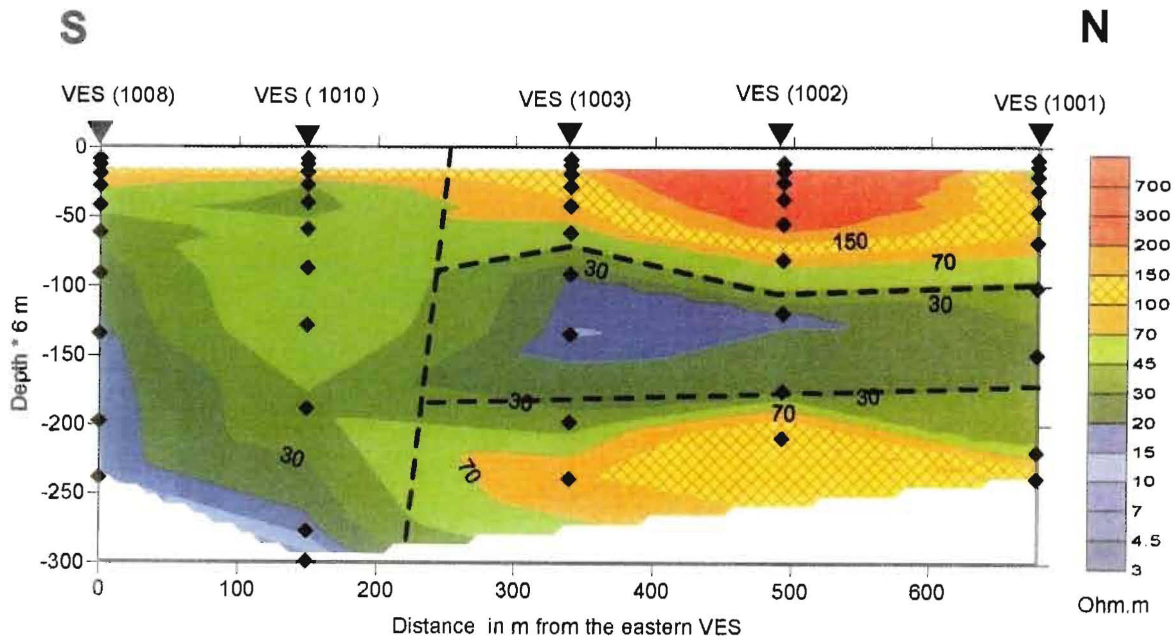

Fig. 9. Resistivity Contour section of Profile AW, along Wadi Lusub, Haddat Ash Sham area.

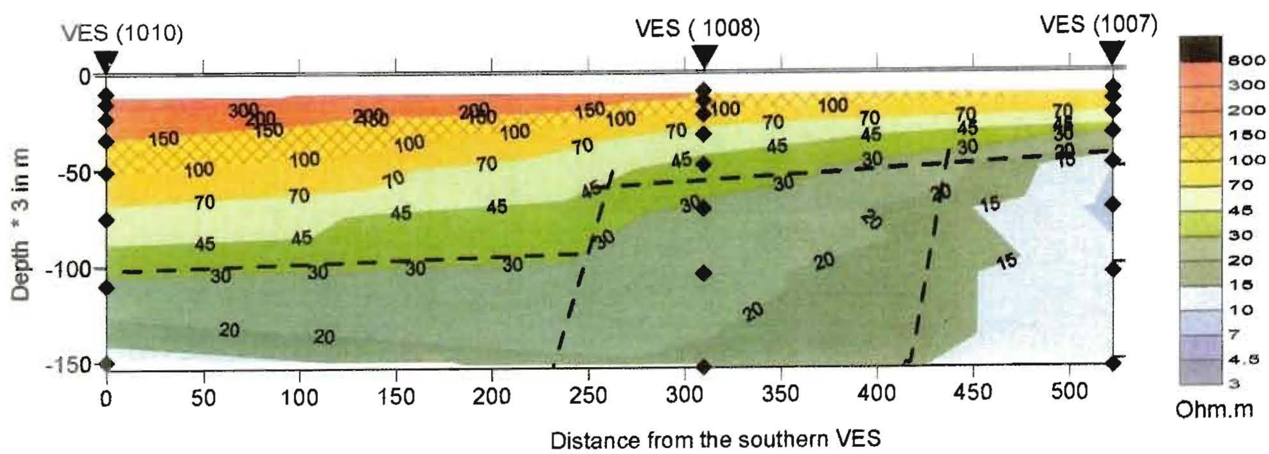

Fig. 10. Resistivity Contour section of Profile Ta, across Wadi Lusub.

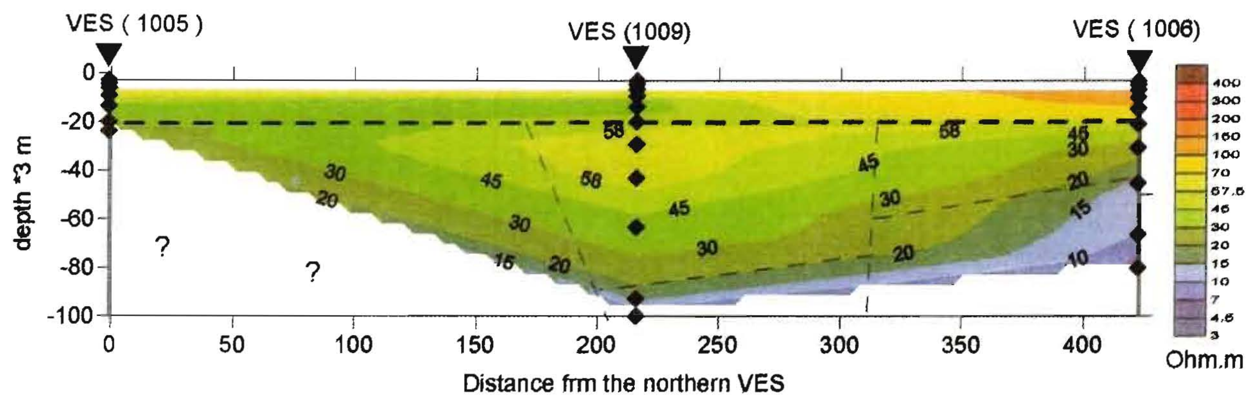

Fig. 11. Resistivity Contour section of Profile Tb, across Wadi Lusub.

El-Dobakhy, (1999) Numerical modeling for evaluation of the groungwater reservoir in the Agriculture Experimental Station in Haddat Ash Sham. M.Sc. thesis, King Abdulaziz Univ.

Ghosh, D.P. (1971) Inverse filter coefficients for the computation of apparent resistivity standard curves for a horizontally stratified earth, Geophys. Prosp. 19: 769-775.

Moore, T.A. and Al-Reheili, M.H. (1989) Geologic map of the Mekkah Quadrangle, Sheet 21D, Kingdom of Saudi Arabia:Saudi Arabia Direcrorate general of mineral resources Geoscience's map GM-107, Scale 1:250,000 with text, 62p.

O'Neill, D.J. (1975) Improved linear filter coefficients for application in apparent resistivity computation, Bull. Aust Sac Exp. Geophys. 6: 104-109.

Reid, A.B., Allsop, J.M., Granser, H., Millet, A. J., and Somerton, I.W. (1990) Magnetic interpretation in the three dimensions using Euler deconvolution; Geophysics, 55, 80-91.

Smith, J. W. (1981) Reconnaissance geologic map of the Wadi Hammah quadrangle, sheet 22/40C, Kingdom of Saudi Arabia: Saudi Arabian Deputy Ministry for minièeral Resources Geologic Map GM-35, scale 1:100,000, with text, 18p.

Ibd. (1982) Reconnaissance geologic map of the Wadi Hammah quadrangle, sheet 22/40C, Kingdom of Saudi Arabia: Saudi Arabian Deputy Ministry for mini\eral Resources Geologic Map GM-65, scale 1:100,000, with text, 19p.

Zeidan, R., and Banat, K. (1990) Petrology, Mineralogy and Geochemestry of the sedimentary formations of Usfan, Haddat Ash Sham and Shumysi areas, and their associatred oolitic ironstone interbeds, North East and East of Jeddah, Saudi Arabia, King AbdulAziz Universty, directorate of Research Projects 035/406/264 p.

Zohdy, A.A. (1974) A computer program for automatic interpretation of Schlumberger sounding curves over horizontal stratified media, U.S. Geological Survey Report, USGS, GD-74-017, PB 232703, 116 p.

Zohdy, A.A. (1975) Automatic interpretation of Schlumberger sounding curves, using modified Dar Zarrouk functions, US Geological Survey Bull. 1313-E, 39 p.

Zohdy, A. A., and Bisdorf, R.J. (1989) Programs for the automatic processing and interpretation of Schlumberger sounding curves in quickBasic 4.0: U.S. Geologic Survey, Open File Report 89-137 A and B, 64 P. + 1 Disk.

Ref: 2331
Received: 14/03/2004
In revised form:15/05/2006